

# Solidification microstructure of laser floating zone remelted Al<sub>2</sub>O<sub>3</sub>/YAG eutectic *in situ* composite

K. Song, J. Zhang, X.J. Jia, H.J. Su\*, L. Liu, H.Z. Fu

State Key Laboratory of Solidification Processing, Northwestern Polytechnical University, Xi'an 710072, PR China

## ARTICLE INFO

### Article history:

Received 11 May 2011

Received in revised form

5 January 2012

Accepted 7 February 2012

Communicated by J.B. Mullin

Available online 17 February 2012

### Keywords:

A1. Crystal morphology

A1. Directional solidification

A1. Eutectics

A2. Floating zone technique

## ABSTRACT

Alumina based eutectic *in situ* composite is now considered to be a promising candidate for ultrahigh temperature structural materials due to its excellent performance even close to its melting point. In this work, Laser Floating Zone (LFZ) solidification experiments have been performed on Al<sub>2</sub>O<sub>3</sub>/Y<sub>2</sub>O<sub>3</sub> containing 18.5 mol% Y<sub>2</sub>O<sub>3</sub> eutectic *in situ* composite at growth rate between 8 and 800 μm/s. The solid/liquid (S/L) interface morphology of this system was reported. Based on the interface morphology, the lamellar selection mechanism of irregular eutectic systems was also discussed. The solidification microstructure evolution was studied, and the characteristic scale of irregular eutectic systems was analyzed using a mathematical model considering non-isothermal interface morphology. An important parameter,  $\Phi$ , which represents relationship between characteristic scales, was also given.

© 2012 Elsevier B.V. All rights reserved.

## 1. Introduction

Directionally solidified Al<sub>2</sub>O<sub>3</sub>/YAG eutectic *in situ* composite has recently been considered as one of the most promising structural materials for the applications in oxidizing environment due to its superior high temperature mechanical properties [1–9]. Its flexural strength is maintained at 360–500 MPa from room temperature up to almost the melting point of about 2100 K. The compression creep strength at 1873 K is about 13 times higher than that of sintered composite with the same composition [1,9]. However, there are still many difficulties for its application. One of the bottlenecks is the poor understanding of the relationship between microstructure and solidification conditions.

For Al<sub>2</sub>O<sub>3</sub>/YAG eutectic system, extensive studies have focused on the relationship between average spacing ( $\lambda_{av}$ ) and solidification rate [2,3,10,11], following the classic equation  $\lambda_{av}V^{1/2}=C$ , where  $C$  is a constant. Epelbaum et al. [3] used a  $\mu$ -PD method to prepare eutectic fibers and found that the average spacing agrees with the inverse-square-root dependence on solidification rate according to  $\lambda_{av}V^{1/2}=10$ , where the units of  $\lambda_{av}$  and  $V$  are μm and μm/s, respectively. However, Su et al. [10] suggested the constant  $C$  equaled to 6.7 for solidification rate by the modified electron beam floating zone melting technique. So the constant  $C$  is variable with different experimental conditions. More importantly, this method is semi-quantitative and experiential. For

the Al<sub>2</sub>O<sub>3</sub>/YAG eutectic system, the relationship between microstructure and solidification conditions still needs to be clarified for its future application.

Since the mechanical properties strongly depend on microstructure and the latter is a reflection of the S/L interface behavior, the lack of interface information leads to substantial difficulties for the analysis of microstructure and the establishment of mathematical models to the final design and the tuning of the structures and properties of the composite. In this paper, the S/L interface morphology of Al<sub>2</sub>O<sub>3</sub>/YAG eutectic system was reported. For description of irregular eutectic microstructure, an analysis based on the average spacing ( $\lambda_{av}$ ) fails to capture important elements of the physics associated with the eutectic spacing selection mechanism [12–17]. In this respect, three kinds of characteristic scales, maximum ( $\lambda_{max}$ ), minimum ( $\lambda_{min}$ ) and average ( $\lambda_{av}$ ) spacings, were measured. The mathematical model, proposed by Magnin and Kurz [14], was adopted to analyze the relationship between different characteristic scales of irregular eutectic systems and processing parameters.

## 2. Experimental

The raw materials were prepared using a mixture of commercial powders of Al<sub>2</sub>O<sub>3</sub> (99.99%) and Y<sub>2</sub>O<sub>3</sub> (99.99%) in the binary (81.5 mol% Al<sub>2</sub>O<sub>3</sub>, 18.5 mol% Y<sub>2</sub>O<sub>3</sub>) eutectic compositions. The oxide powders were mechanically mixed by wet ball milling with an aqueous solution of polyvinyl alcohol to obtain a homogeneous slurry and then dried at 473 K in air for 1 h. Afterward, the 68 × 4 × 4 mm<sup>3</sup>

\* Corresponding author. Tel.: +86 29 88492228; fax: +86 29 88494080.  
E-mail address: shjnpu@yahoo.com.cn (H.J. Su).

bar precursors were prepared by uniaxial die pressing at 25 MPa for 10 min, followed by pressureless sintering at 1673 K for 2 h to increase the density and provide handling strength. The laser floating zone melting experiments were carried out under the Ar atmosphere with a laser power of about 400 W, a solidification rate of 8–800  $\mu\text{m/s}$  and a beam diameter of 3 mm. Because the pulling rate is equivalent to solidification rate, all of the following description uses solidification rate. The quenched solid–liquid interface was obtained by abruptly turning off the laser. The directionally solidified eutectic rods with waved surface and high density could be obtained.

The solidified samples were ground with SiC abrasive paper and polished sequentially with diamond paste down to 0.5  $\mu\text{m}$  size. The sample surfaces were coated with a thin layer of Au before observation. The microstructure and component of the composite were determined by scanning electron microscopy (SEM) (JSM-5800), energy dispersive spectroscopy (EDS) (Link-Isis) and x-ray diffraction (XRD) (Rigakumsg-158) technique.

The lamellar spacing was evaluated by scanning the cross-sectional images along a line chosen by eye as perpendicular to most of the phase domains traversed, and then calculating the number of identical pixels (gray or black) in successive segments along the line [18–20]. At least,  $\lambda$  values were measured from 400–500 different areas.  $\lambda_{\text{max}}$ ,  $\lambda_{\text{min}}$  and  $\lambda_{\text{av}}$  were obtained by the arithmetic average of the maximum 20%, minimum 20% and all of the measured values, respectively.

### 3. Results and discussion

XRD and EDS analyses indicate that the binary eutectic microstructure only includes  $\text{Al}_2\text{O}_3$  (black area) and YAG (gray area) without any other metastable phases. As can be seen in Fig. 1, the microstructure of  $\text{Al}_2\text{O}_3/\text{YAG}$  *in situ* composite shows interpenetrating network, like “Chinese script”, in which  $\text{Al}_2\text{O}_3$  phase and YAG phase are three-dimensionally and continuously connected to each other and finely coupled without grain boundaries between interfaces. As expected, the typical microstructure of directionally solidified  $\text{Al}_2\text{O}_3/\text{YAG}$  eutectic system is irregular. The eutectic structure tends to exhibit irregular morphology when the

composition phases possess higher entropy of fusion, typically  $\Delta S/R_g > 5$ , where  $\Delta S$  is the entropy of fusion and  $R_g$  is the gas constant [21]. For  $\text{Al}_2\text{O}_3/\text{YAG}$  system, both of the composition phases have high entropies of fusion ( $\Delta S_{\text{Al}_2\text{O}_3} = 47.72 \text{ J/K mol}$  [22] and  $\Delta S_{\text{YAG}} = 122.38$  [23]). Hence, the microstructure exhibits irregular characteristic under normal growth conditions. In addition, cellular morphology occurs when solidification rate is greater than 200  $\mu\text{m/s}$  and the inter-cell area consists of  $\text{Al}_2\text{O}_3$ . The direct evidence is shown by the arrows in Fig. 1, and the similar phenomenon is also observed in Sn–Cd system [24]. In higher solidification rate, the planar lamellar structure breaks down into a cellular structure, in which a cell can span several hundred lamellar. This is due to constitutional undercooling that develops because of the presence of an impurity enrichment at the interface, formed as a result of the rejection of the impurity by both phases into the liquid. This leads to a simultaneous destabilization of both phases. Furthermore, the solidification rate strongly affects the size of domains of eutectic microstructure. The lamellar spacing decreases rapidly with the increasing rate. The experimental data of  $\lambda_{\text{max}}$ ,  $\lambda_{\text{min}}$  and  $\lambda_{\text{av}}$  were shown in Fig. 2.

Fig. 3 shows the S/L interface morphology of  $\text{Al}_2\text{O}_3/\text{YAG}$  system. It can be seen that both phases develop at the same pace and exhibit coupled growth, and it is hard to distinguish which phase plays a leading role. This finding is different from that in Al–Si [25] and Fe–C [26] systems. As can be seen in Fig. 3b, the lamellar couples with smaller spacing project into the melt due to lower undercooling. Another possible reason is that a short period of rapid growth which is contributed by switching off the laser induces to smaller lamellar spacing. We can also infer two mechanisms of lamellar selection from the observation of the morphology of the interface: branching and ceasing. In Fig. 3c, the arrows represent the solidification directions of two lamellas. When two lamellae converge, the lamellar spacing will decrease to  $\lambda_{\text{ex}}$  which has been identified in JH model [21]. The spacing cannot further reduce since this will lead to the increase of undercooling. In this case, the growth of one phase simply stops, thereby increasing spacing. Therefore,  $\lambda_{\text{ex}}$  can be regarded as the lowest bound of the value of the irregular eutectic spacing. Conversely, when the lamellar spacing is much larger than  $\lambda_{\text{ex}}$ ,

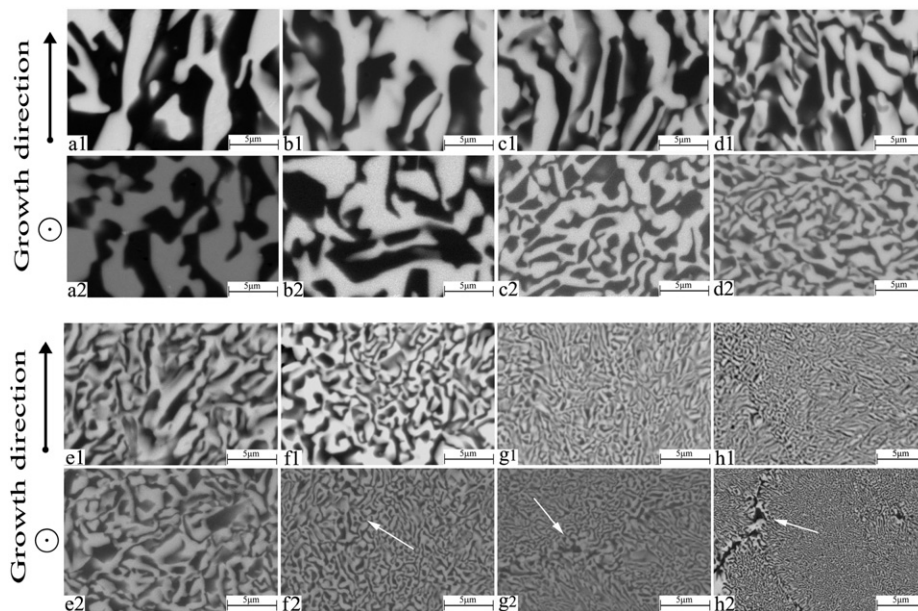


**Fig. 1.** Variation of lamellar spacing at the different  $V$  of  $\text{Al}_2\text{O}_3/\text{YAG}$  *in situ* composite: (a1) longitudinal section, (a2) transverse sections ( $V=8 \mu\text{m/s}$ ); (b1) longitudinal section, (b2) transverse sections ( $V=16 \mu\text{m/s}$ ); (c1) longitudinal section, (c2) transverse sections ( $V=30 \mu\text{m/s}$ ); (d1) longitudinal section, (d2) transverse sections ( $V=50 \mu\text{m/s}$ ); (e1) longitudinal section, (e2) transverse sections ( $V=100 \mu\text{m/s}$ ); (f1) longitudinal section, (f2) transverse sections ( $V=200 \mu\text{m/s}$ ); (g1) longitudinal section, (g2) transverse sections ( $V=400 \mu\text{m/s}$ ); (h1) longitudinal section, (h2) transverse section ( $V=800 \mu\text{m/s}$ ).

Download English Version:

<https://daneshyari.com/en/article/1791737>

Download Persian Version:

<https://daneshyari.com/article/1791737>

[Daneshyari.com](https://daneshyari.com)